ATP homeostasis underlies optimal glucose consumption by *Saccharomyces cerevisiae*

Kulika Chomvong[1], Daniel I. Benjamin[2], Daniel K. Nomura[2] and Jamie H.D. Cate[3,4,5,#]

[1]Department of Plant and Microbial Biology, University of California, Berkeley, CA 94720

[2]Department of Nutritional Sciences and Toxicology, University of California, Berkeley, CA 94720

[3]Department of Molecular and Cell Biology, University of California, Berkeley, CA 94720

[4]Department of Chemistry, University of California, Berkeley, CA 94720

[5]Physical Biosciences Division, Lawrence Berkeley National Laboratory, Berkeley, CA 94720

[#]Corresponding author (email: jcate@lbl.gov)

KC: kchomv@gmail.com

DIB: dbenjami@stanford.edu

DKN: dnomura@berkeley.edu

JHDC: jcate@lbl.gov

Running title: ATP and optimal glucose consumption

Final character count: 50,759

Keywords: cellobiose/GCN4/glucose sensors/metabolomics/PMA1

23

24 ## Abstract

25

26 Glycolysis is central to energy metabolism in most organisms, and is highly
27 regulated to enable optimal growth. In the yeast *Saccharomyces cerevisiae*, feedback
28 mechanisms that control flux through glycolysis span transcriptional control to
29 metabolite levels in the cell. Using a cellobiose consumption pathway, we decoupled
30 glucose sensing from carbon utilization, revealing new modular layers of control that
31 induce ATP consumption to drive rapid carbon fermentation. Proton pumping and
32 regulation of amino acid biosynthesis mediated by extracellular glucose sensors
33 independently contribute to maintenance of energy homeostasis. Controlling the upper
34 bound of cellular ATP levels may be a general mechanism used to regulate energy
35 levels in cells, via a regulatory network that can be uncoupled from ATP concentrations
36 under perceived starvation conditions.

37

38

Introduction

Most microorganisms favor glucose as their primary carbon source, as reflected in their genetic programs hard-wired for this preference. Central to carbon metabolism is glycolysis, which is finely tuned to the dynamic state of the cell due to the fact that glycolysis first consumes ATP before generating additional ATP equivalents. To avoid catastrophic depletion of ATP, the yeast *Saccharomyces cerevisiae* has evolved a transient ATP hydrolysis futile cycle coupled to gluconeogenesis (van Heerden *et al*, 2014). Glycolysis in yeast is also tightly coupled to glucose transport into the cell, entailing three extracellular glucose sensing mechanisms and at least one intracellular glucose signaling pathway (Youk & van Oudenaarden, 2009).

Synthetic biology and metabolic engineering of yeast holds promise to convert this microorganism into a “cell factory” to produce a wide range of chemicals derived from renewable resources or those unattainable through traditional chemical routes. However, many applications require tapping into metabolites involved in central carbon metabolism, a daunting challenge as living cells have numerous layers of feedback regulation that fine-tune growth to changing environments. Cellular regulation evolved intricate networks to maintain and ensure cell survival. For example *S. cerevisiae* has evolved to rapidly consume high concentrations of glucose through fermentation, while repressing the expression of other carbon consumption pathways, an effect termed glucose repression. When perturbed genetically, regulatory networks such as those in glucose repression often generate undesirable or unexpected phenotypes.

For yeast to be useful in producing large volumes of renewable chemicals or biofuels, it will be important to expand its carbon utilization to include multiple sugars in the plant cell wall. One promising approach that helps overcome glucose repression and allows simultaneous utilization of different sugars is cellobiose consumption (Ha *et al*, 2011). Cellobiose is a disaccharide with two units of glucose linked by a ß-1,4 glycosidic bond. Cellobiose consumption using a minimal additional pathway in yeast—a cellodextrin transporter (CDT-1) and intracellular ß-glucosidase (Galazka *et al*, 2010)–avoids glucose repression by importing carbon in the form of cellobiose instead of glucose. The cellodextrin transporter allows cellobiose to enter the cell where it is hydrolyzed to glucose and consumed via the native glycolytic consumption pathway. By moving glucose production into the cell, the *N. crassa*-derived cellobiose consumption pathway is nearly the minimal synthetic biological module imaginable in *S. cerevisiae*, comprised of just two genes. Nevertheless, in *S. cerevisiae* the cellobiose consumption pathway is inferior to consumption of extracellular glucose in terms of rate and results in a prolonged lag phase (Lin *et al*, 2014). Previous efforts to understand the impact of cellobiose consumption on the physiology of *S. cerevisiae* using transcriptional profiling revealed that cellobiose improperly regulates mitochondrial activity and amino acid biosynthesis, both of which are tightly coupled to the transition from respiration to fermentation (Lin *et al*, 2014).

Since glycolytic enzymes are regulated mostly at the post-transcriptional level (Daran-Lapujade *et al*, 2007), we probed cellobiose consumption in *S. cerevisiae* at the metabolite level. We found that key metabolites in glycolysis are highly imbalanced, leading to low flux through glycolysis and slow fermentation. We also found that excess

ATP levels drive the imbalance, and identified a new regulatory role of glucose sensors in cellular ATP homeostasis.

Results

Metabolite profiling of cellobiose utilizing *S. cerevisiae*

S. cerevisiae cells engineered with the cellobiose consumption pathway ferment cellobiose more slowly than glucose and often exhibit a prolonged lag phase when transitioning to consumption of this disaccharide (Lin *et al*, 2014). We hypothesized that cellobiose consumption results in an ATP deficit in glycolysis relative to glucose, due to the fact that the cellodextrin transporter (CDT-1) in the cellobiose utilizing pathway is a proton symporter, requiring ATP hydrolysis for cellobiose uptake (Kim *et al*, 2014). Moreover, under anaerobic conditions, ATP production is limited to substrate-level phosphorylation, further restricting ATP availability. We measured the steady-state concentrations of ATP and other metabolites in central carbon metabolism in yeast fermenting cellobiose compared to glucose. Of the 48 compounds analyzed, the abundance of 25 compounds was significantly different (p-value < 0.01) between cellobiose and glucose-fed samples (Figure 1A). Surprisingly, ATP levels increased by 6-fold in the cellobiose grown cells (Figure 1B). The relative abundance of compounds in glycolysis—fructose 6-phosphate (F6P), glucose 6-phosphate (G6P), glucose and pyruvate—increased by 444-, 81-, 7- and 3-fold, respectively, while that of phosphoenolpyruvate decreased by 2-fold (Figure 1B). These results suggest that the

yeast cells underwent drastic physiological changes, reflected in metabolite levels, when cellobiose was provided in place of glucose.

Phosphofructokinase-1 inhibition by excess ATP

Given the dramatic buildup of glucose, G6P and F6P intermediates prior to the phosphofructokinase (*PFK1*) reaction in glycolysis (Figure 2A), we reasoned that Pfk1 might be a major bottleneck in cellobiose consumption. Pfk1 catalyzes the phosphorylation of F6P, using one ATP and yielding fructose 1,6-bisphosphate (F1,6BP) as a product. As the second committed step in glycolysis, Pfk1 is heavily regulated—with ATP acting as an allosteric inhibitor and AMP and fructose 2,6-bisphosphate serving as activators (Bañuelos *et al*, 1977; Avigad, 1981; Nissler *et al*, 1983).

To test whether allosteric inhibition of Pfk1 by ATP limited cellobiose fermentation, a mutation in Pfk1 that makes the enzyme ATP-insensitive (P722L in the Pfk1 beta subunit, note the original publication referred to this mutation as P728L (Rodicio *et al*, 2000)) was introduced into the chromosomally encoded *PFK1* gene (mutation here termed *pfk1m*) in the cellobiose utilizing strain. This mutation was previously shown to reduce ATP inhibition but also AMP and fructose 2,6-bisphosphate activation of Pfk1 in *S. cerevisiae* (Rodicio *et al*, 2000). We chose this mutation over an ATP-insensitive, AMP/F2,6BP-sensitive mutant phosphofructokinase (Nissler *et al*, 1983) because the latter's phenotype has not been evaluated in *S. cerevisiae*. Consistent with allosteric inhibition of Pfk1 by ATP, the cellobiose consumption efficiency (E_c) of the *pfk1m* strain increased by 33% in comparison to the strain with

wild-type Pfk1 (Figure 2B). Furthermore, the relative abundance of G6P and F1,6BP decreased by 47% and 34%, respectively, while that of ATP remained relatively unchanged (Figure 2C). These results indicate that the 6-fold increase in cellular ATP concentrations allosterically inhibited Pfk1, resulting in accumulation of glucose, G6P and F6P, which eventually slowed down cellobiose consumption.

Limited activity of plasma membrane ATPase

Although the *pfk1m* strain partially increased the rate of cellobiose fermentation, cellular ATP remained elevated relative to glucose fermentation. It is unlikely that ATP production was the cause of the difference, as fermentation is limited to substrate-level phosphorylation under anaerobic conditions regardless of carbon source. We therefore tested whether the activity of one of the major ATP sinks in yeast, the plasma membrane ATPase (Pma1) was responsible for the ATP buildup. Pma1 hydrolyzes 25-40% of cellular ATP in yeast (Gradmann *et al*, 1978) and is heavily regulated by glucose (Serrano, 1983).

A constitutively active mutant form of *PMA1* (*pma1*-Δ916, here abbreviated *pt*) (Mason *et al*, 2014) was introduced into the endogenous *PMA1* locus in the cellobiose utilizing strain. This mutation results in high Pma1 ATPase activity even in carbon starvation conditions (Mason *et al*, 2014). We observed a 66% decrease in cellular ATP levels in the *pt* strain in comparison to the wild-type control (WT, i.e. cellobiose pathway only) (Figure 2C). Phenotypically, the E_c of the mutant strain was 4 times that of the control (Figure 2B). In addition, the concentrations of G6P and F1,6BP decreased by 58% and 93%, respectively, relative to strains expressing wild-type *PMA1*. Notably,

these concentrations dropped more than when the ATP-insensitive *PFK1* mutant was introduced (Figure 2C). These results suggest that increased Pma1 ATPase activity improved cellobiose fermentation, by alleviating ATP accumulation that allosterically inhibited Pfk1 in glycolysis.

With decreased intracellular ATP concentrations in the *pma1*-Δ916 strain, ATP inhibition at the Pfk1 step is unlikely to limit glycolysis. Consistent with this hypothesis, the cellobiose consumption profile of a *pfk1m-pt* double mutant was identical to that of the *pt* strain (Figure 2A). Surprisingly, the levels of G6P, F1,6BP and ATP in the double mutant strain were higher than in the *pt* strain (Figure 2C). In fact, their levels were similar to those in the *pfk1m* strain (Figure 2C). This may be because *pfk1m* has reduced activation by AMP and fructose 2,6-bisphosphate, in addition to reduced inhibition by high ATP concentrations (Rodicio *et al*, 2000). Taken together, these data suggest that the effect of reduced Pfk1 allosteric activation may only be evident in the absence of Pfk1 inhibition by ATP.

Carbon starvation-like state of the plasma membrane ATPase

We wondered whether the limited Pma1 activity in cellobiose-fed cells is due to the absence of extracellular glucose in the media. Transcriptionally, the presence of glucose increases *PMA1* mRNA levels by 2-4 times via the regulation of Rap1, Gcr1 and Sir2 (Rao *et al*, 1993; García-Arranz *et al*, 1994; Kang *et al*, 2015). Consistent with the requirement for extracellular glucose sensing, previous RNA sequencing experiments revealed a 40% decrease in *PMA1* transcript levels when cellobiose was provided in place of glucose (Lin *et al*, 2014). However, although transcriptional

regulation of *PMA1* is important, it is slower than post-transcriptional regulation and results in smaller changes (Serrano, 1983; Eraso *et al*, 2006). In the presence of glucose, phosphorylation of Ser-899 decreases Pma1's K_m and Ser-911/Thr-912 increases Pma1's V_{max} for ATP, respectively (Serrano, 1983; Portillo *et al*, 1991; Lecchi *et al*, 2007). Given the excess amount of ATP observed in cellobiose utilizing conditions (Figure 1), we hypothesized that V_{max}-determining phosphorylation states of Ser-911 and Thr-912 might play a major role in establishing the efficiency of cellobiose fermentation. We did not investigate the phosphorylation of Ser-899, because the 6-fold excess of ATP likely overcame the potential problems associated with K_m values (Eraso & Portillo, 1994).

Combinatorial mutations of Ser-911/Thr-912 to alanine and aspartic acid were introduced into the endogenous *PMA1* gene to prevent or mimic phosphorylation, respectively. We were unable to obtain strains with *pma1* S911A T912A and *pma1* S911A T912D, potentially because the combinations were lethal. All mutant strains whose Pma1 S911 position was mutated to aspartic acid consumed cellobiose more efficiently in comparison to when the S911 position remained unchanged (Figure 3A). By contrast, mutating Pma1 T912 to aspartic acid did not show a correlation with the cellobiose consumption phenotype. These results suggest that phosphorylation of Pma1 at S911 was lacking when cellobiose was provided as a sole carbon source.

Positive effects of extracellular glucose sensor deletions

According to the above mutational analysis, the Pma1 phosphorylation state of cellobiose-fed cells was similar to that in carbon starvation conditions (Figure

3B) (Lecchi *et al*, 2007). Based on the relatively high level of intracellular glucose present in the cellobiose-grown cells (Figure 1), extracellular glucose is likely to be essential for full activation of Pma1 through S911 phosphorylation, as high intracellular glucose concentrations (Figure 1) or glucose metabolism (Rolland *et al*, 2002) was unable to satisfy this role.

Snf3, Rgt2 and Gpr1 are the three known sensors of extracellular glucose in *S. cerevisiae*. Snf3 and Rgt2 mainly regulate glucose transport while Gpr1 controls cell physiology via an interaction with Gpa2 to activate protein kinase A and cAMP synthesis (Rolland *et al*, 2002). To mimic the presence of extracellular glucose, constitutively active mutations (*snf3* R229K, *rgt2* R231K and *gpa2* R273A) were introduced into the endogenous loci to probe the role of each glucose-sensing pathway (Ozcan *et al*, 1996; Xue *et al*, 1998). Surprisingly, the cellobiose consumption efficiency of all the three mutant strains decreased by ~25% (Figure S1A). We then inverted the genetic modifications by deleting *SNF3, RGT2* and/or *GPA2*. Notably, the triple glucose-sensing deletion strain (*snf3*Δ*rgt2*Δ*gpa2*Δ, *or srg*Δ) showed a 275% increase in E_c (Figure 4A).

Combinatorial deletions revealed that the Gpr1 pathway did not contribute to improved cellobiose fermentation, but combining the *SNF3* and *RGT2* deletions (*sr*Δ) was necessary and sufficient to replicate the E_c of the triple deletion strain (Figure 4A, Figure S1C). Consistent with the observed E_c values, the intracellular ATP levels of *srg*Δ and *sr*Δ decreased by 41% and 18% respectively, while those in the individual-deletion strains *snf3*Δ and *rgt2*Δ remained unchanged (Figure 4A). These results reveal a negative correlation between E_c and cellular ATP levels (Figure 4B) and that Snf3 and

Rgt2 acted together to regulate cellular ATP levels, in addition to regulating glucose transport.

Although the additional deletion of *GPA2* (*gpa2*Δ) in the *sr*Δ strain did not further improve E_c (Fig 4A), it reduced the relative abundance of ATP by 28%, implying that the Gpr1 pathway has a separate mechanism to control cellular ATP levels that does not directly affect carbon metabolism. Consistently, *gpa2*Δ had a negative or neutral impact on cellobiose consumption (Figure S1). The decrease in ATP level may be a result of altered cellular activities, controlled by Gpr1 via the Tor and cAMP-PKA-Ras pathways (Rolland *et al*, 2002). The relationship between Gpr1-regulated ATP levels and carbon metabolism remains to be discovered. Since *gpa2*Δ did not have a direct effect on E_c, it was not investigated further in this study.

Snf3/Rgt2 regulation of cellular ATP levels

To examine whether Snf3/Rgt2 regulated the cellular ATP level in cellobiose fermentations via Pma1, an *snf3*Δ *rgt2*Δ *pma1-*Δ*916* strain (*sr*Δ*-pt*) was constructed. Notably, the E_c of the *sr*Δ*-pt* strain increased more than 4 times in comparison to the wild-type control (Figure 4A, C). The improvement was additive, within the range of the ΔE_c summation of *sr*Δ and *pma1-*Δ*916* strains relative to wild-type (Figure 4C). Although ATP levels decreased in a nearly linear fashion as a function of E_c (Figure 4B), it is not presently possible to ascertain whether the *sr*Δ and *pma1-*Δ*916* mutations act entirely independently due to limitations in measurement accuracy (Figure 4C).

To further determine the relationship between Snf3/Rgt2 and Pma1, the vanadate-specific ATPase activity of Pma1 (Viegas & Sá-Correia, 1991) from different

strains consuming cellobiose were analyzed (Figure 5). Consistent with the constitutively active nature of the *pt* mutation, the activities of Pma1 in the *pt* and *sr*Δ-*pt* strains were higher than those observed in the WT or *sr*Δ strains, respectively. Notably, the ATPase activitiy of Pma1 in *sr*Δ was comparable to the WT strain suggesting that Snf3 and Rgt2 in combination do not regulate Pma1 transcriptionally or post-translationally in a straightforward manner.

Transcriptional impact of Snf3/Rgt2 Deletion

Given the lower cellular ATP concentration (Figure 4A) but nearly unchanged Pma1 ATPase activity in the *sr*Δ strain relative to WT (Figure 5), Snf3/Rgt2 likely regulate ATP homeostasis through an additional mechanism other than Pma1. A systems-level analysis of yeast transcriptomes from the WT, *s*Δ, *r*Δ, and *sr*Δ strains identified 137 genes that were differentially expressed and unique to *sr*Δ (p-value < 0.001 and absolute fold change > 2 for *sr*Δ compared pairwise with WT, *s*Δ and *r*Δ) (Dataset 1.3). Notably, 14 genes (10.2%) encoding ATP binding proteins and those involved in ATP catabolic processes were upregulated (Figure S2, Dataset 1.4). The 137 genes were further categorized into five clusters (Dataset 1.5), revealing upregulation of genes involved in cellular amino acid biosynthesis, metabolic processes and ATP catabolic processes, and downregulation of those in phospholipid biosynthesis, phospholipid metabolism, mitochondrial structure, negative regulation of gluconeogenesis and translation initiation factor eIF1 (SUI1) (Dataset 1.5, Figure S2). A more comprehensive analysis of genes involved in amino acid biosynthesis revealed a

high correlation with upregulation of Gcn4, the central transcriptional activator of genes in this pathway (Figure S3, Dataset 1.7) (Moxley *et al*, 2009; Natarajan *et al*, 2001).

Discussion

To identify the effects of a minimal alteration to carbon metabolism in yeast, we chose a cellobiose-consumption pathway composed of two genes and analyzed its cellular metabolite profiles in comparison to cells provided with glucose, yeast's preferred carbon source (Figure 6). Cellobiose consumption efficiency (E_c) linearly correlated with ethanol production rate, while ethanol yield remained mostly unchanged (Figure S4).

More than half of the metabolites changed abundance significantly when cellobiose was provided in place of glucose. The buildup of G6P, F6P and ATP in *S. cerevisiae* fermenting cellobiose suggested that Pfk1 was one of the bottlenecks in the process. Pfk1 is subjected to complex allosteric regulation, including inhibition by ATP and activation by AMP and fructose 2,6-bisphosphate (F2,6BP) (Bañuelos *et al*, 1977; Avigad, 1981; Nissler *et al*, 1983). The Pfk1 bottleneck was partially relieved in cells expressing an ATP/AMP/F2,6BP-insensitive *PFK1* allele, while the ATP level remained elevated. These results contrast with previous studies that identified ATP depletion and the buildup of fructose-1,6-bisphosphate–the metabolite immediately downstream of Pfk1–as a weak link in glycolysis (van Heerden *et al*, 2014). Although we did not investigate the effect of AMP and F2,6BP activation since their changes between glucose and cellobiose conditions were less than 2 fold and not statistically significant

(p-value ≥ 0.01), it is possible that they could influence cellobiose consumption efficiency.

Although ATP is central to a cell's energy currency, too much ATP is not necessary beneficial (Pontes *et al*, 2015; Browne, 2013). In fact, we observed a negative correlation between cellular ATP levels and cellobiose consumption efficiency (Figure 4B). A similar correlation has been reported for glucose as a carbon source, suggesting metabolic uncoupling of energy homeostasis in yeast cells (Larsson *et al*, 1997). We propose that intracellular glucose concentrations–generated by cellobiose hydrolysis in our experiments–and glucose metabolism (Rolland *et al*, 2002) are insufficient to trigger glucose activation of key metabolic pathways and enzyme activity. For example, we found that the ATP-dependent proton pump Pma1 existed in a carbon-starvation like state during cellobiose fermentation, and was partially responsible for the aberrant accumulation of ATP. These results suggest that neither intracellular glucose nor glucose metabolism are sufficient to fully activate Pma1. A previous study showed the lack of phosphorylation of S899 and S911/T912 in Pma1, in a hexokinase/glucokinase deletion strain (*hxk1*Δ *hxk2*Δ *glk1*Δ) provided with glucose, suggesting that phosphorylation of these residues requires glucose metabolism (Mazón *et al*, 2015). Together with our results, we propose that the activation of Pma1 through S911 phosphorylation requires both extracellular glucose and glucose metabolism. Our results reveal that the cellobiose utilization system allows uncoupling of glucose metabolism and intracellular glucose from extracellular glucose signaling. Future experiments will be required to reveal why ATP was not consumed by other cellular processes triggered under starvation (Thomsson *et al*, 2003).

Cytosolic pH is also a key regulator of carbon utilization (Dechant & Peter, 2014), and is likely to be impacted by the use of the proton symporter CDT-1 for cellobiose import and the resulting low activity of Pma1. High cytosolic pH is necessary and sufficient to activate Tor-Ras-PKA activities, which are downstream of Gpr1 glucose sensing pathway (Dechant & Peter, 2014). By contrast, the proton symporter CDT-1 and low activity of Pma1 may result in a low cytosolic pH. However, cytosolic pH alone is unlikely to determine the cellobiose consumption efficiency (E_c) as the strain with an ATP/AMP/F2,6BP-insensitive *PFK1* allele showed improved E_c but unaltered cellular ATP levels. Furthermore, the inactivation of the Gpr1 pathway resulted in decreased cellular ATP but unaltered E_c. Glucose storage, i.e. in the form of trehalose, may be interconnected through the Gpr1 pathway because Ras-cAMP activates trehalase required to break down trehalose—a phenomenon observed when gluconeogenesis is switched to glycolysis (Thevelein & Hohmann, 1995). Trehalose cycling has been shown to lead to an imbalanced state of glycolysis (van Heerden *et al*, 2014). The relationship between carbon storage and E_c will require future studies to examine this relationship.

We also found that the well-studied extracellular glucose sensors Snf3/Rgt2 exhibited a novel role in cellular ATP homeostasis through an unknown mechanism, which seems to be independent of the major plasma membrane ATPase Pma1. Deletion of extracellular glucose sensors (Snf3/Rgt2) increased cellobiose consumption efficiency and partially restored ATP levels. It is known that deletion of *SNF3* and *RGT2* slows down glucose consumption (Choi *et al*, 2015), due to the inability of these strains to degrade Mth1/Std1, which block the promoter regions of hexose transporters

required for optimal glucose import (Moriya & Johnston, 2004; Flick *et al*, 2003; Lakshmanan *et al*, 2003; Jouandot *et al*, 2011). Unlike glucose, cellobiose does not signal Mth1 degradation even with intact Snf3/Rgt2 (Jouandot *et al*, 2011). Thus, genes downstream of Mth1 regulation, including hexose transporters, are not expected to be responsible for the improved E_c and decreased cellular ATP levels observed in *sr*Δ. Based on transcriptome profiling, the lack of Snf3 and Rgt2 increases ATP-requiring cellular activities through regulatory nodes other than Mth1. Consistent with this model, no growth defect is observed in a *mth1*Δ strain growing on glucose, suggesting that Snf3/Rgt2 has additional regulatory nodes other than Mth1 (Choi *et al*, 2015).

Regulation of ATP levels by the combined action of Snf3 and Rgt2 seems to involve transcriptional activation of amino acid biosynthetic pathways (Figure S3), although Snf3 and Rgt2 are glucose sensors (Rolland *et al*, 2002). In yeast, general amino acid control (GAAC) requires transcription factor Gcn4, which directly activates the amino acid biosynthetic pathways, as well as pathways for vitamins associated with amino acid synthesis in conditions of amino acid starvation or stress (Natarajan *et al*, 2001; Moxley *et al*, 2009). Notably, the transcription profile of the *srΔ* strain compared to WT reveals that pathways directly regulated by Gcn4 are induced during cellobiose fermentation, indicating that Gcn4 is activated in these conditions (Figure S3). Interestingly, we found that patterns of transcription activation of wild-type *GCN4* relative to *gcn4*Δ strains correlate highly with *srΔ* relative to WT in cellobiose fermentations (correlations of 0.52 with (Moxley *et al*, 2009) and 0.68 with (Natarajan *et al*, 2001),respectively) (Figure S3).

The present results indicate that Snf3 and Rgt2 repress Gcn4 levels in the absence of glucose. *GCN4* mRNA levels remain unchanged in *srΔ* relative to WT, indicating that Gcn4 repression by Snf3 and Rgt2 also likely occurs translationally (Hinnebusch, 1997).These results come as a surprise, as previous experiments showed glucose limitation induced *GCN4* mRNA translation as a starvation response (Yang *et al*, 2000). Glucose limitation was shown to activate *GCN4* mRNA translation by stimulating Gcn2 kinase activity (Yang *et al*, 2000), which is responsible for phosphorylating translation initiation factor eIF2 and depleting active ternary complexes of eIF2 with initiator tRNA and GTP (Hinnebusch, 1997). By contrast, a chemical genetics approach identified the kinase Snf1, the yeast homologue of human AMP-activated protein kinase (AMPK), as a repressor of *GCN4* mRNA translation in conditions with a non-glucose sugar and abundant amino acid availability (Shirra *et al*, 2008), conditions more in line with those used here.

As a homolog of the important energy sensor AMPK that maintains energy homeostasis in the cells (Hardie, 2011), it is tempting to speculate that Snf1 plays a role in ATP regulation downstream of Snf3/Rgt2, and potentially connects to Gcn4. Snf1 is required for expression of glucose-repressed genes and may be regulated by mitochondrial starvation signaling (Li *et al*, 2013). Mitochondrial activation observed in cellobiose fermentation compared to glucose fermentation (Lin *et al*, 2014) may be a readout of the Snf1 regulation. The direct relationships between Snf3/Rgt2, Snf1, Gcn4, mitochondrial activation and cellular ATP remains to be investigated.

One possible additional mechanism of activation of *GCN4* mRNA translation could be depletion of translation initiation factor 1 (eIF1, encoded by *SUI1*). In the *srΔ*

strain, levels of *SUI1* mRNA decreased nearly 2.6-fold. Consistent with a direct role for eIF1, previous results demonstrated that activation of *GCN4* translation decreases with increased functional eIF1 levels (Hinnebusch, 1997; Herrmannová *et al*, 2012). Notably, *SUI1* transcript levels were also lower in *GCN4* cells when compared to *gcn4Δ* strains in starvation conditions (Natarajan *et al*, 2001). Future experiments will be required to demonstrate a direct link between eIF1 levels and *GCN4* mRNA translation activation.

The present systems-level study of a minimal synthetic biology pathway for cellobiose consumption revealed the dramatic impact of decoupling extracellular and intracellular glucose sensing, resulting in an overabundance of ATP in cells. The inability of *S. cerevisiae* to catabolize ATP for cellular processes in the presence of intracellular glucose and glucose metabolism but in the absence of extracellular glucose resulted in slow fermentation. Thus, ATP levels must be kept in a relatively narrow range for optimal fermentation and to allow robust startup of glycolysis, yet yeast seems to lack a direct mechanism to monitor ATP concentrations. For example, a dynamic model showed that a small concentration difference of inorganic phosphate, a product of ATP hydrolysis, could alter cell fate from a stable glycolytic steady state to an imbalanced dead-end state (van Heerden *et al*, 2014). Here, we found that the extracellular glucose sensing by Snf3/Rgt2 required for optimal glucose fermentation (Youk & van Oudenaarden, 2009) can be uncoupled from the role of these receptors in regulating ATP homeostasis under carbon starvation conditions. It will be important in the future to map the fully regulatory pathways of ATP homeostasis leading from Snf3/Rgt2 and, independently, terminating in Pma1, along with the mechanisms

connecting carbon utilization to the translation of the master transcriptional regulator Gcn4.

Materials & Methods

Yeast strains, media and anaerobic fermentation

The *S. cerevisiae* background strain used in this study was S288C *ura3::*P_{PGK1}*-cdt-1* N209S/F262Y-T_{ADH1} *lyp1::*P_{TDH3}*-gh1-1 (codon optimized)-*T_{CYC1} derived by chromosomal DNA library selection (Ryan *et al*, 2014). The strain was subjected to further modifications using the CRISPRm system (Ryan *et al*, 2014). The list of strains constructed, CRISPRm guides and primers used are included in Table S1.

Seed cultures for cellobiose fermentation experiments were grown in 20 g/L glucose modified optimal minimal media (oMM) (Lin *et al*, 2014) and harvested at mid-log phase. All cellobiose fermentation experiments were conducted under strict anaerobic conditions, in 80 g/L cellobiose oMM media at an initial OD_{600} of 20, using 10 mL serum flasks containing 5 mL fermentation in 2-5 biological replicates. The flasks were incubated at 30°C, 220 rpm. The cellobiose consumption efficiency (E_c) was defined as the inverse of the area under the curve of extracellular cellobiose concentration over time.

Analytical analysis of yeast metabolites

Extracellular cellobiose concentrations were determined by high performance liquid chromatography on a Prominence HPLC (Shimadzu, Kyoto, Japan) equipped with

Rezex RFQ-FastAcid H 10 x 7.8 mm column. The column was eluted with 0.01 N of H_2SO_4 at a flow rate of 1 mL/min, 55°C.

For the metabolite profiling comparison between glucose and cellobiose (modified from (Benjamin *et al*, 2014)) , equal amounts of yeast cells at mid-exponential phase of anaerobic sugar consumption (10 g/L cellobiose or glucose) were harvested (final pellet OD_{600} equivalent to 5). The samples were quenched in 180 µL of 40:40:20 acetonitrile:methanol:water. Following the addition of 10 nmols of d3 serine (as an internal standard), the mixtures were vortexed and centrifuged at 13,000 rpm for 10 minutes. The supernatants were injected onto an Agilent 6460 QQQ LC-MS/MS and the chromatography was achieved by normal phase separation with a Luna NH_2 column (Phenomenex) starting with 100% acetonitrile with a gradient to 100% 95:5 water acetonitrile. 0.1% formic acid or 0.2% ammonium hydroxide with 50 mM ammonium acetate was added to assist with ionization in positive and negative ionization mode, respectively. Five biological replicates were used for each sample analyzed.

For targeted intracellular metabolite comparisons, yeast cells equivalent to 20 OD_{600} units were harvested and filtered through a 0.8 µm nylon membrane, prewashed with 3 mL water, followed by another 3 mL water wash after cell filtration. The membranes were placed in 1.5 mL extraction solution (0.1 M formic acid, 15.3 M acetonitrile) flash-frozen in liquid nitrogen, and stored at -80°C. Before analysis, the extracts were vortexed for 15 minutes and centrifuged to collect the supernatants at 4°C. Glucose 6-phosphate and fructose 1,6-bisphosphate were separated and identified using a 1200 Series liquid chromatography instrument (Agilent Technologies, Santa Clara, CA). 1 µL of each sample was injected onto an Agilent Eclipse XDB-C18 (2.1 mm

i.d., 150 mm length, 3.5 µm particle size) column with a Zorbax SB-C8 (2.1 mm i.d., 12.5 mm length, 5 µm particle size) guard column and eluted at 25 °C and a flow rate of 0.2 mL/min with the following gradient (modification from (Luo *et al*, 2007)): 15 min isocratic 100% buffer A (10 mM tributylamine/15 mM acetic acid), then in 15 min with a linear gradient to 60% buffer B (methanol), 2 min isocratic 60% B, then 10 min equilibration with 100% buffer A. The eluent from the column was introduced into a mass spectrometer for 25 minutes after the first 10 minutes. Mass spectrometry (MS) was performed on an LTQ XL ion trap instrument (Thermo Fisher Scientific, San Jose, CA) with an ESI source operated in negative ion mode. The MS settings were capillary temperature 350 °C, ion spray voltage 4.5 kV, sheath gas flow: 60 (arbitrary units), auxiliary gas flow 10 (arbitrary units), sweep gas flow 5 (arbitrary units). For the MS/MS product ion scan, the scan range was m/z 80 to m/z 300. The compounds G6P at m/z 259.1 and F16BP at m/z 339.1 were isolated with an m/z 2 isolation width and fragmented with a normalized collision-induced dissociation energy setting of 35% and with an activation time of 30 ms and an activation Q of 0.250.

Plasma membrane isolation

Strains were subjected to cellobiose fermentation under anaerobic conditions. Yeast cells with an OD_{600} equivalent to 40 were harvested at mid-log phase and flash frozen in liquid nitrogen. Membrane fractions were extracted based on the protocol published in (Kaiser *et al*, 2002).

Pma1 ATPase activity assay

The ATPase assay described in (Viegas & Sá-Correia, 1991) was modified as follows. 30 µg of the isolated membrane fraction was incubated in assay buffer (50 mM MES pH 5.7, 10 mM $MgSO_4$, 50 mM KCl, 5 mM NaN_3, 50 mM KNO_3) with and without 3 mM orthovanadate for 25 minutes at 30 °C. 1.8 mM ATP was added to start the 100 uL reactions. The reactions were incubated at 30 °C for 15 minutes, then the membranes were isolated from the reactions by centrifugation at 13,000x g for 10 minutes at 4°C. The released inorganic phosphate was measured in the supernatant using the ATPase/GTPase Activity Assay Kit (Sigma-Aldrich) based on the manufacturer's protocol. The specific Pma1 ATPase activities were calculated by subtracting the concentration of released inorganic phosphate in reactions provided with orthovanadate from those without.

RNA Sequencing

Total RNA was extracted from yeast cells equivalent to 40 OD_{600} units harvested at mid exponential phase by the RiboPure Yeast kit (Thermo Fisher Scientific). Multiplexed libraries were then derived from the total RNA using TruSeq RNA Library Preparation Kits v2 (Illumina Sequencing). The quality of the library was evaluated by Agilent Bioanalyzer 2000 (Functional Genomics Laboratory, UC Berkeley) and sequenced with Illumina HiSeq2500 RAPID platform (Vincent J. Coates Genomic Sequencing Laboratory, UC Berkeley). The reads were assembled and analyzed in CLC Genomics Workbench 9 (Denmark). RPKM (Reads Per Kilobase of exon model per Million mapped reads) was chosen as the expression value output, which was

490 further normalized by the total expression values in a sample. Functional classification
491 was performed using FunSpec (Robinson *et al*, 2002).
492
493 **Yeast cell-based cellobiose uptake assay**
494 The cell-based cellobiose uptake assay was modified from (Li *et al*, 2015). Yeast
495 strains were grown to mid-exponential phase in 2% oMM glucose, washed with assay
496 buffer (5 mM MES, 100 mM NaCl, pH 6.0) three times and resuspended to a final OD_{600}
497 of 10. Equal volumes of the cell suspension and 200 μM cellobiose were mixed to start
498 the reactions, which were incubated at 30°C with continuous shaking for 15 minutes.
499 The reactions were stopped by adding 150 μL of supernatants to 150 μL 0.1 M NaOH.
500 The concentrations of the remaining cellobiose were measured using an ICS-3000 Ion
501 Chromatography System (Dionex, Sunnyvale, CA, USA) equipped with a CarboPac®
502 PA200 carbohydrate column. The column was eluted with a NaOAc gradient in 100 mM
503 NaOH at a flow rate of 0.4 mL/min, 30°C.
504
505 **Acknowledgements**
506 The authors thank Dr. Xin Li, Dr. Ligia Acosta-Sampson, Dr. Yuping Lin and Dr.
507 Matt Shurtleff for helpful discussions. This work was supported by funding from Energy
508 Biosciences Institute to JHDC and from National Institutes of Health (R01CA172667) to
509 DKN.
510
511 **Conflict of Interest**
512 The authors declare that they have no conflict of interest.

Author contributions

All authors contributed to the design of the experiments. KC and DIB carried out the experiments. DKN and JHDC aided in interpretation of the systems-level experiments. KC wrote the manuscript, with editing from DIB, DKN, and JDHC.

References:

Avigad G (1981) Stimulation of yeast phosphofructokinase activity by fructose 2,6-bisphosphate. *Biochem. Biophys. Res. Commun.* **102:** 985–991

Bañuelos M, Gancedo C & Gancedo JM (1977) Activation by phosphate of yeast phosphofructokinase. *J. Biol. Chem.* **252:** 6394–6398

Benjamin DI, Louie SM, Mulvihill MM, Kohnz RA, Li DS, Chan LG, Sorrentino A, Bandyopadhyay S, Cozzo A, Ohiri A, Goga A, Ng S-W & Nomura DK (2014) Inositol phosphate recycling regulates glycolytic and lipid metabolism that drives cancer aggressiveness. *ACS Chem. Biol.* **9:** 1340–1350

Browne SE (2013) When too much ATP is a bad thing: a pivotal role for P2X7 receptors in motor neuron degeneration. *J. Neurochem.* **126:** 301–304

Choi K-M, Kwon Y-Y & Lee C-K (2015) Disruption of Snf3/Rgt2 glucose sensors decreases lifespan and caloric restriction effectiveness through Mth1/Std1 by adjusting mitochondrial efficiency in yeast. *FEBS Lett.* **589:** 349–357

Daran-Lapujade P, Rossell S, van Gulik WM, Luttik MAH, de Groot MJL, Slijper M, Heck AJR, Daran J-M, de Winde JH, Westerhoff HV, Pronk JT & Bakker BM (2007) The fluxes through glycolytic enzymes in Saccharomyces cerevisiae are predominantly regulated at posttranscriptional levels. *Proceedings of the National Academy of Sciences* **104:** 15753–15758

Dechant R & Peter M (2014) Cytosolic pH: A conserved regulator of cell growth? *Mol Cell Oncol* **1:** e969643–4

Eraso P & Portillo F (1994) Molecular mechanism of regulation of yeast plasma membrane H(+)-ATPase by glucose. Interaction between domains and identification of new regulatory sites. *J. Biol. Chem.* **269:** 10393–10399

Eraso P, Mazón MJ & Portillo F (2006) Yeast protein kinase Ptk2 localizes at the plasma membrane and phosphorylates in vitro the C-terminal peptide of the H+-ATPase. *Biochimica et Biophysica Acta (BBA) - Biomembranes* **1758:** 164–170 Available at: http://www.sciencedirect.com/science/article/pii/S0005273606000125

546 Flick KM, Spielewoy N, Kalashnikova TI, Guaderrama M, Zhu Q, Chang H-C &
547 Wittenberg C (2003) Grr1-dependent inactivation of Mth1 mediates glucose-induced
548 dissociation of Rgt1 from HXT gene promoters. *Molecular Biology of the Cell* **14:**
549 3230–3241

550 Galazka JM, Tian C, Beeson WT, Martinez B, Glass NL & Cate JHD (2010) Cellodextrin
551 transport in yeast for improved biofuel production. *Science* **330:** 84–86

552 García-Arranz M, Maldonado AM, Mazón MJ & Portillo F (1994) Transcriptional control
553 of yeast plasma membrane H(+)-ATPase by glucose. Cloning and characterization
554 of a new gene involved in this regulation. *J. Biol. Chem.* **269:** 18076–18082

555 Gradmann D, Hansen UP, Long WS, Slayman CL & Warncke J (1978) Current-voltage
556 relationships for the plasma membrane and its principal electrogenic pump in
557 Neurospora crassa: I. Steady-state conditions. *J. Membr. Biol.* **39:** 333–367

558 Ha S-J, Galazka JM, Kim SR, Choi J-H, Yang X, Seo J-H, Glass NL, Cate JHD & Jin Y-
559 S (2011) Engineered Saccharomyces cerevisiae capable of simultaneous cellobiose
560 and xylose fermentation. *Proc. Natl. Acad. Sci. U.S.A.* **108:** 504–509

561 Hardie DG (2011) AMP-activated protein kinase: an energy sensor that regulates all
562 aspects of cell function. *Genes Dev.* **25:** 1895–1908

563 Herrmannová A, Daujotyte D, Yang J-C, Cuchalová L, Gorrec F, Wagner S, Dányi I,
564 Lukavsky PJ & Valásek LS (2012) Structural analysis of an eIF3 subcomplex
565 reveals conserved interactions required for a stable and proper translation pre-
566 initiation complex assembly. *Nucleic Acids Res.* **40:** 2294–2311

567 Hinnebusch AG (1997) Translational regulation of yeast GCN4. A window on factors
568 that control initiator-trna binding to the ribosome. *J. Biol. Chem.* **272:** 21661–21664

569 Jouandot D, Roy A & Kim J-H (2011) Functional dissection of the glucose signaling
570 pathways that regulate the yeast glucose transporter gene (HXT) repressor Rgt1. *J.*
571 *Cell. Biochem.* **112:** 3268–3275

572 Kaiser CA, Chen EJ & Losko S (2002) Subcellular fractionation of secretory organelles.
573 *Meth. Enzymol.* **351:** 325–338

574 Kang WK, Kim YH, Kang HA, Kwon K-S & Kim J-Y (2015) Sir2 phosphorylation through
575 cAMP-PKA and CK2 signaling inhibits the lifespan extension activity of Sir2 in yeast.
576 *Elife* **4:**

577 Kim H, Lee W-H, Galazka JM, Cate JHD & Jin Y-S (2014) Analysis of cellodextrin
578 transporters from Neurospora crassa in Saccharomyces cerevisiae for cellobiose
579 fermentation. *Appl. Microbiol. Biotechnol.* **98:** 1087–1094

580 Lakshmanan J, Mosley AL & Ozcan S (2003) Repression of transcription by Rgt1 in the
581 absence of glucose requires Std1 and Mth1. *Curr. Genet.* **44:** 19–25

582 Larsson C, Nilsson A, Blomberg A & Gustafsson L (1997) Glycolytic Flux Is
583 Conditionally Correlated with ATP Concentration in. *J. Bacteriol.* **179:** 7243–7250

584 Lecchi S, Nelson CJ, Allen KE, Swaney DL, Thompson KL, Coon JJ, Sussman MR &
585 Slayman CW (2007) Tandem phosphorylation of Ser-911 and Thr-912 at the C
586 terminus of yeast plasma membrane H+-ATPase leads to glucose-dependent
587 activation. *J. Biol. Chem.* **282:** 35471–35481

588 Li L, Chen Y & Gibson SB (2013) Starvation-induced autophagy is regulated by
589 mitochondrial reactive oxygen species leading to AMPK activation. *Cell. Signal.* **25:**
590 50–65

591 Li X, Yu VY, Lin Y, Chomvong K, Estrela R, Park A, Liang JM, Znameroski EA, Feehan
592 J, Kim SR, Jin Y-S, Glass NL & Cate JHD (2015) Expanding xylose metabolism in
593 yeast for plant cell wall conversion to biofuels. *Elife* **4:**

594 Lin Y, Chomvong K, Acosta-Sampson L, Estrela R, Galazka JM, Kim SR, Jin Y-S &
595 Cate JH (2014) Leveraging transcription factors to speed cellobiose fermentation by
596 Saccharomyces cerevisiae. *Biotechnology for Biofuels* **7:** 126

597 Luo B, Groenke K, Takors R, Wandrey C & Oldiges M (2007) Simultaneous
598 determination of multiple intracellular metabolites in glycolysis, pentose phosphate
599 pathway and tricarboxylic acid cycle by liquid chromatography-mass spectrometry. *J*
600 *Chromatogr A* **1147:** 153–164

601 Mason AB, Allen KE & Slayman CW (2014) C-terminal truncations of the
602 Saccharomyces cerevisiae PMA1 H+-ATPase have major impacts on protein
603 conformation, trafficking, quality control, and function. *Eukaryotic Cell* **13:** 43–52

604 Mazón MJ, Eraso P & Portillo F (2015) Specific phospho-antibodies reveal two
605 phosphorylation sites in yeast Pma1 in response to glucose. *FEMS Yeast Res.*

606 Moriya H & Johnston M (2004) Glucose sensing and signaling in Saccharomyces
607 cerevisiae through the Rgt2 glucose sensor and casein kinase I. *Proceedings of the*
608 *National Academy of Sciences* **101:** 1572–1577

609 Moxley JF, Jewett MC, Antoniewicz MR, Villas-Boas SG, Alper H, Wheeler RT, Tong L,
610 Hinnebusch AG, Ideker T, Nielsen J & Stephanopoulos G (2009) Linking high-
611 resolution metabolic flux phenotypes and transcriptional regulation in yeast
612 modulated by the global regulator Gcn4p. *Proc. Natl. Acad. Sci. U.S.A.* **106:** 6477–
613 6482

614 Natarajan K, Meyer MR, Jackson BM, Slade D, Roberts C, Hinnebusch AG & Marton
615 MJ (2001) Transcriptional profiling shows that Gcn4p is a master regulator of gene
616 expression during amino acid starvation in yeast. *Mol. Cell. Biol.* **21:** 4347–4368

617 Nissler K, Otto A, Schellenberger W & Hofmann E (1983) Similarity of activation of
618 yeast phosphofructokinase by AMP and fructose-2,6-bisphosphate. *Biochem.*

Biophys. Res. Commun. **111:** 294–300

Ozcan S, Dover J, Rosenwald AG, Wolfl S & Johnston M (1996) Two glucose transporters in Saccharomyces cerevisiae are glucose. *Proceedings of the National Academy of Sciences* **93:** 12428–12432

Pontes MH, Sevostyanova A & Groisman EA (2015) When Too Much ATP Is Bad for Protein Synthesis. *J. Mol. Biol.* **427:** 2586–2594

Portillo F, Eraso P & Serrano R (1991) Analysis of the regulatory domain of yeast plasma membrane H+-ATPase by directed mutagenesis and intragenic suppression. *FEBS Lett.* **287:** 71–74

Rao R, Drummond-Barbosa D & Slayman CW (1993) Transcriptional regulation by glucose of the yeast PMA1 gene encoding the plasma membrane H(+)-ATPase. *Yeast* **9:** 1075–1084

Robinson MD, Grigull J, Mohammad N & Hughes TR (2002) FunSpec: a web-based cluster interpreter for yeast. *BMC Bioinformatics* **3:** 35

Rodicio R, Strauss A & Heinisch JJ (2000) Single point mutations in either gene encoding the subunits of the heterooctameric yeast phosphofructokinase abolish allosteric inhibition by ATP. *J. Biol. Chem.* **275:** 40952–40960

Rolland F, Winderickx J & Thevelein JM (2002) Glucose-sensing and -signalling mechanisms in yeast. *FEMS Yeast Res.* **2:** 183–201

Ryan OW, Skerker JM, Maurer MJ, Li X, Tsai JC, Poddar S, Lee ME, DeLoache W, Dueber JE, Arkin AP & Cate JHD (2014) Selection of chromosomal DNA libraries using a multiplex CRISPR system. *Elife* **3:**

Serrano R (1983) In vivo glucose activation of the yeast plasma membrane ATPase. *FEBS Lett.* **156:** 11–14

Shirra MK, McCartney RR, Zhang C, Shokat KM, Schmidt MC & Arndt KM (2008) A chemical genomics study identifies Snf1 as a repressor of GCN4 translation. *J. Biol. Chem.* **283:** 35889–35898

Thevelein JM & Hohmann S (1995) Trehalose synthase: guard to the gate of glycolysis in yeast? *Trends Biochem. Sci.* **20:** 3–10

Thomsson E, Larsson C, Albers E, Nilsson A, Franzén CJ & Gustafsson L (2003) Carbon starvation can induce energy deprivation and loss of fermentative capacity in Saccharomyces cerevisiae. *Appl. Environ. Microbiol.* **69:** 3251–3257

van Heerden JH, Wortel MT, Bruggeman FJ, Heijnen JJ, Bollen YJM, Planque R, Hulshof J, O'Toole TG, Wahl SA & Teusink B (2014) Lost in Transition: Start-Up of Glycolysis Yields Subpopulations of Nongrowing Cells. *Science* **343:** 1245114–

654 1245114 Available at: http://www.sciencemag.org/cgi/doi/10.1126/science.1245114

655 Viegas CA & Sá-Correia I (1991) Activation of plasma membrane ATPase of
656 Saccharomyces cerevisiae by octanoic acid. *J. Gen. Microbiol.* **137:** 645–651

657 Xue Y, Batlle M & Hirsch JP (1998) GPR1 encodes a putative G protein-coupled
658 receptor that associates with the Gpa2p Galpha subunit and functions in a Ras-
659 independent pathway. *EMBO J.* **17:** 1996–2007

660 Yang R, Wek SA & Wek RC (2000) Glucose limitation induces GCN4 translation by
661 activation of Gcn2 protein kinase. *Mol. Cell. Biol.* **20:** 2706–2717

662 Youk H & van Oudenaarden A (2009) Growth landscape formed by perception and
663 import of glucose in yeast. *Nature* **462:** 875–879

664

665

Figure Legends

Figure 1. Metabolite profile of cells provided with glucose or cellobiose. (A) Heatmap representation of steady state intracellular metabolite abundance of cells provided with glucose or cellobiose under anaerobic conditions. Shown are the results of 5 biological replicates. * identified compounds that were significantly different between glucose and cellobiose conditions (p-value < 0.01) (B) Significant changes of intracellular metabolite levels in cells provided with cellobiose compared to cells provided glucose as a sole carbon source (p-value < 0.01 and fold-change >2, five biological replicates).

Figure 2. Manipulation of phosphofructokinase (*PFK1*) and plasma membrane ATPase *(PMA1*). (A) Schematic representation of cellobiose consumption route in the upper glycolytic pathway. Glc, G6P, F6P and ATP are highlighted, and were found in higher abundance when cellobiose was provided in comparison to glucose. (B) Cellobiose consumption profile of the strains with ATP-insensitive Pfk1 (*pfk1m*), constitutively active Pma1 (*pt*) and the combination of both mutations (*pfk1m-pt*) in comparison to the cellobiose pathway-only strain, here used as wild-type (WT). (C) Relative abundance of G6P, F1,6BP and ATP levels of the WT, *pfk1m, pt* and *pfk1m-pt* strains, relative to the WT strain fermenting cellobiose. The experiments were carried out in 5 biological replicates, with standard errors from the mean shown.

Figure 3. Carbon starvation-like state of the plasma membrane ATPase (*PMA1*) in cellobiose-fermenting cells. (A) Cellobiose consumption efficiency (E_c) of cells expressing Pma1 with phosho-mimic or phosphorylation-preventing mutations at

positions serine 911 (S911) and threonine 912 (T912). Shown are the mean and standard deviation for 3 biological replicates. (B) Phosphorylation states of Pma1 S911 and T912 under carbon starvation, glucose metabolizing and cellobiose metabolizing conditions. The experiments were carried out in 2 biological replicates, with standard errors from the mean shown.

Figure 4. Effect of glucose sensor deletions. (A) Cellobiose consumption efficiency (E_c) and cellular ATP levels of strains with different glucose sensor deletions and different combinations of constitutively-active Pma1 mutations. Shown are the averages and standard deviations of three biological replicates. (B) Correlation of E_c and cellular ATP. Standard deviations for three biological replicates are shown for each point. (C) Additive effect of the increase in E_c and the decrease in cellular ATP of *sr*Δ and *pt* in *sr*Δ-*pt* strain. The experiments were carried out in 5 biological replicates, with standard errors form the mean shown.

Figure 5. ATPase activity of the plasma membrnae ATPase Pma1. Specific Pma1 ATPase of WT, *pt, sr*Δ and *sr*Δ-*pt* strains measured from normalized membrane fractions of cells harvested at mid-log phase. The experiments were carried out in 3 biological replicates, with standard errors from the mean shown.

Figure 6. Schematic representation of ATP homeostasis and cellular regulation of cellobiose fermentation. Excess ATP inhibited phosphofructokinase (Pfk1), resulting in an upper glycolytic metabolite buildup and slow cellobiose consumption. The buildup of ATP may be caused by low activity of Pma1, with no phosphorylation at position 911. Additionally, glucose sensors Snf3 and Rgt2 together influenced cellular ATP levels via

709 Gcn4-regulated amino acid biosynthesis.

710

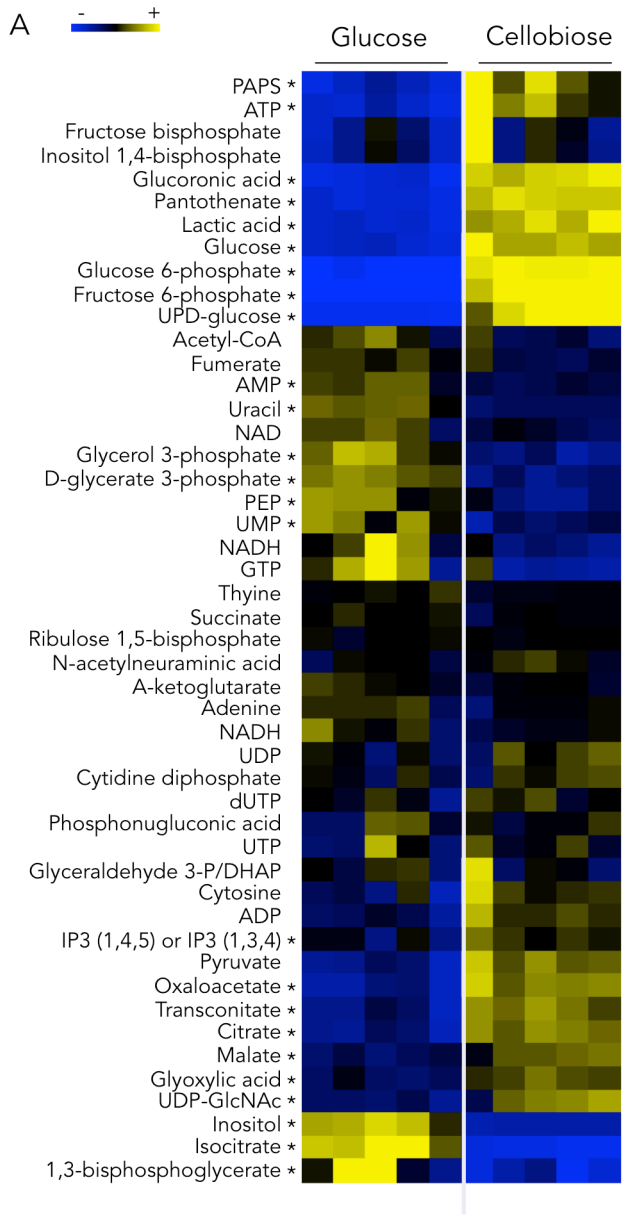

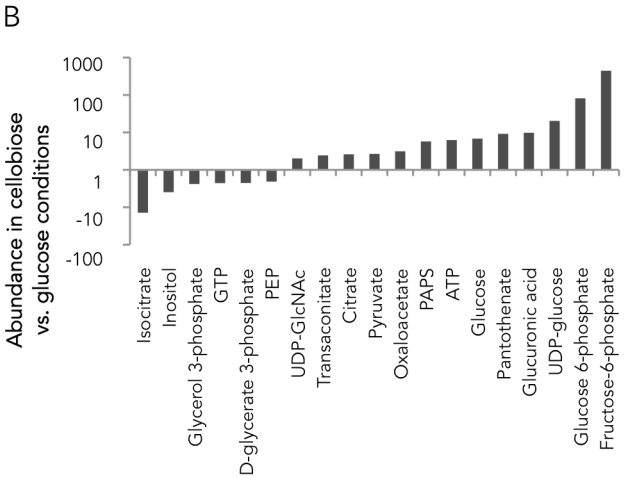

710

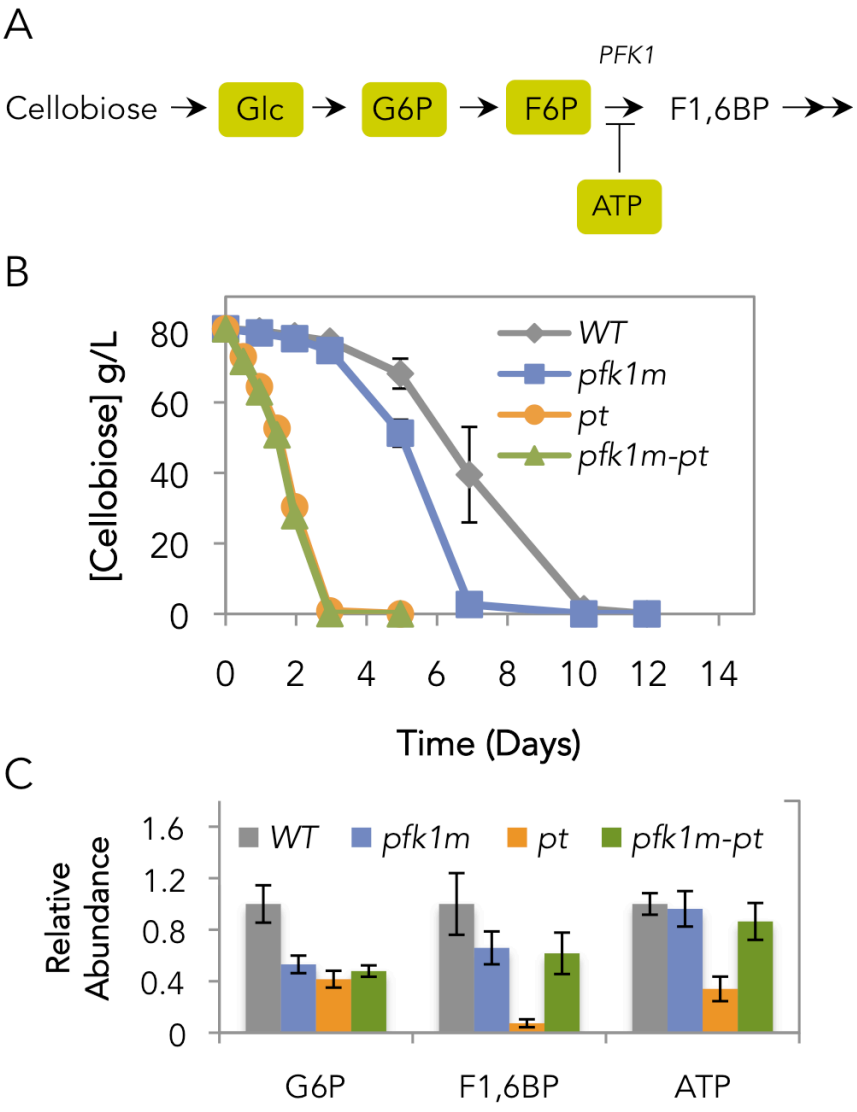

711
712

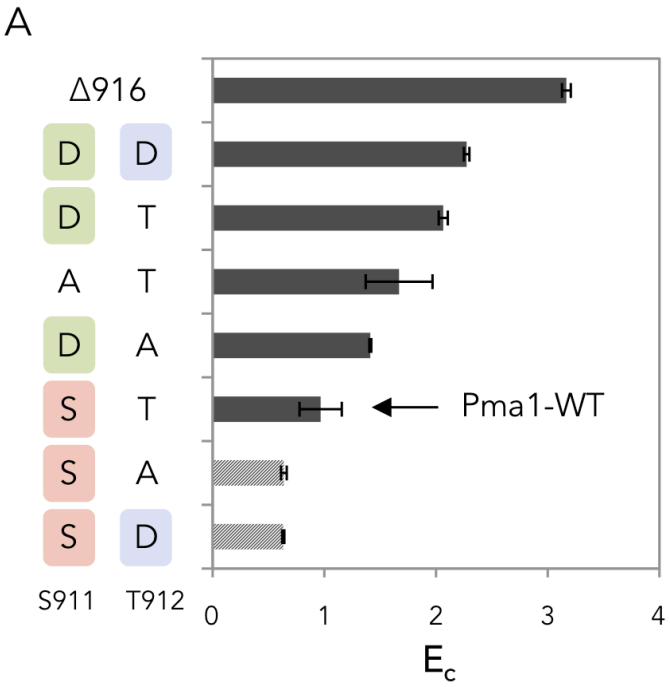

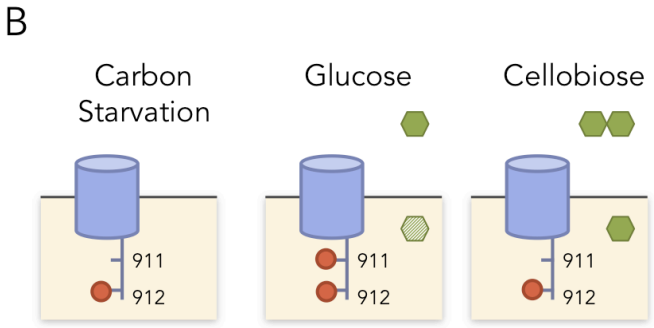

712
713

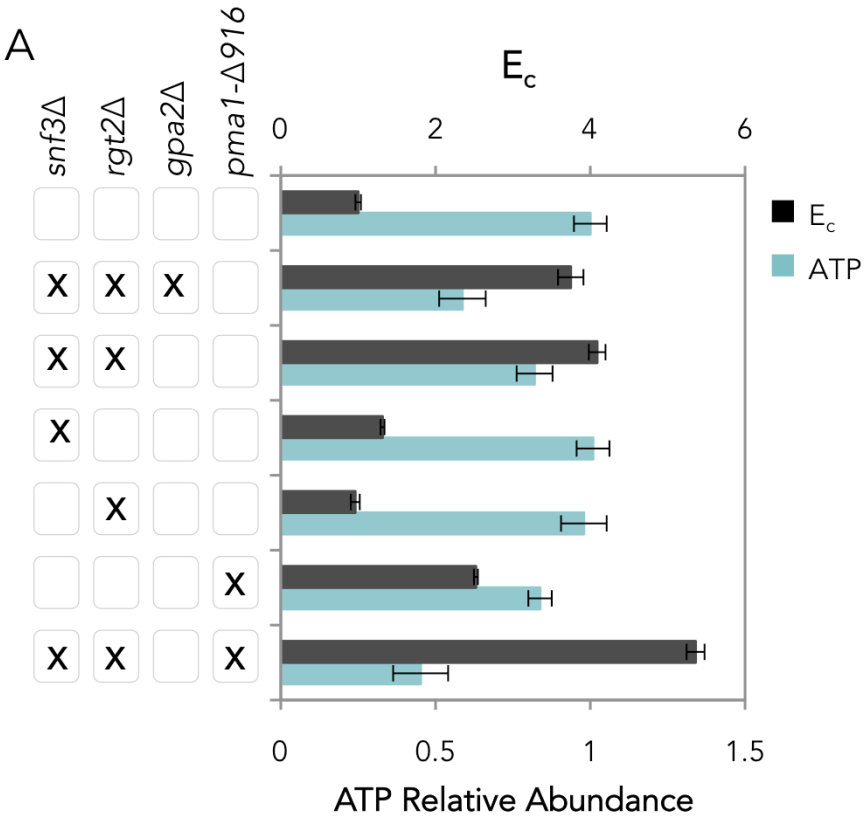

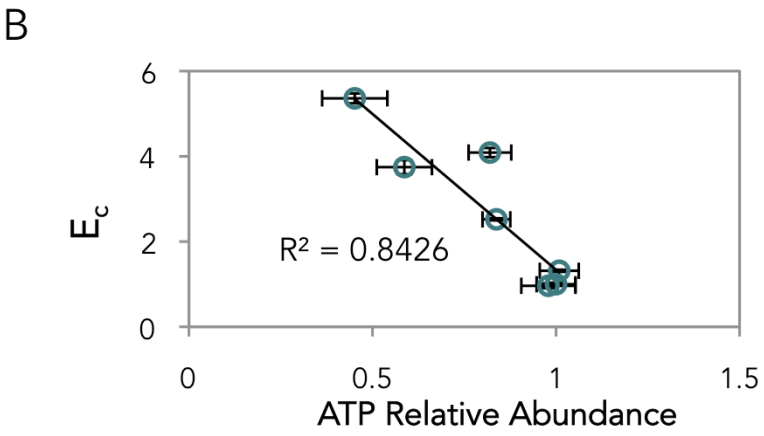

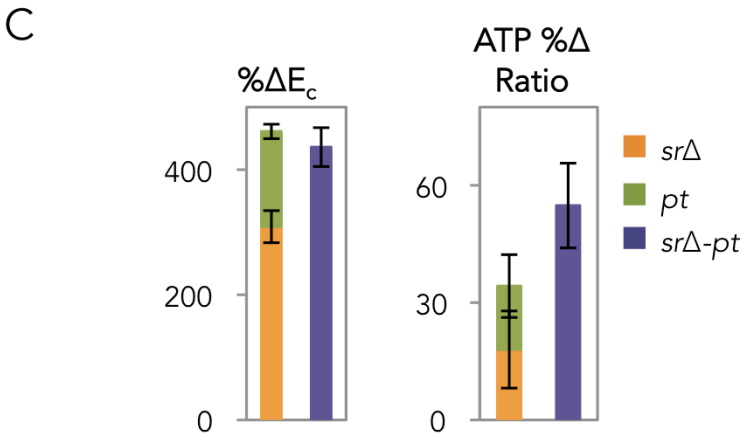

713

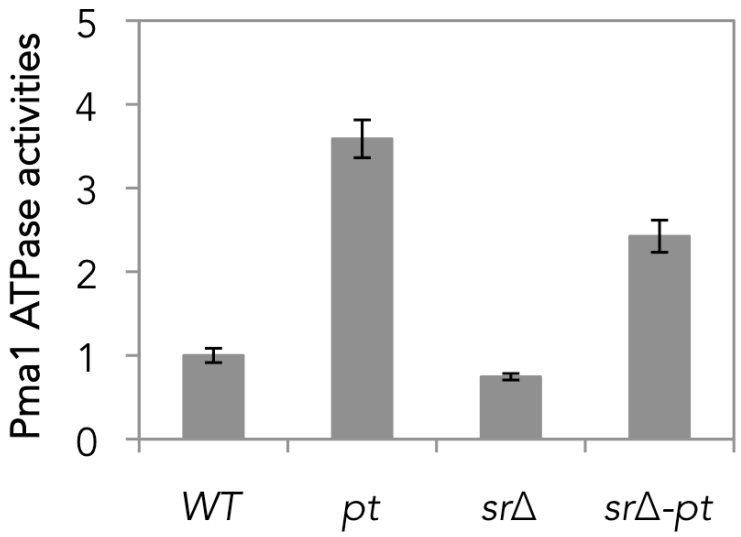

714
715

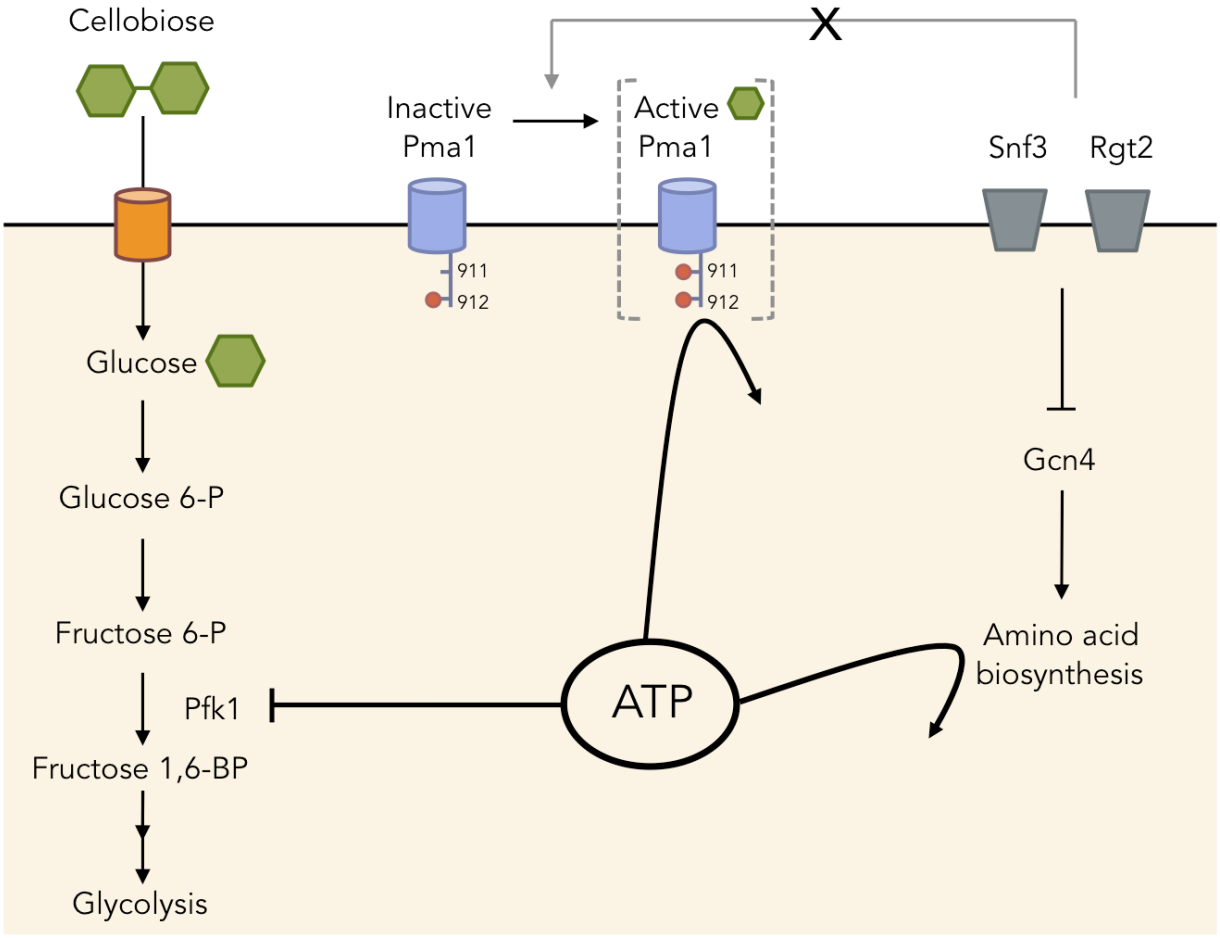

715
716

Supplementary Figures

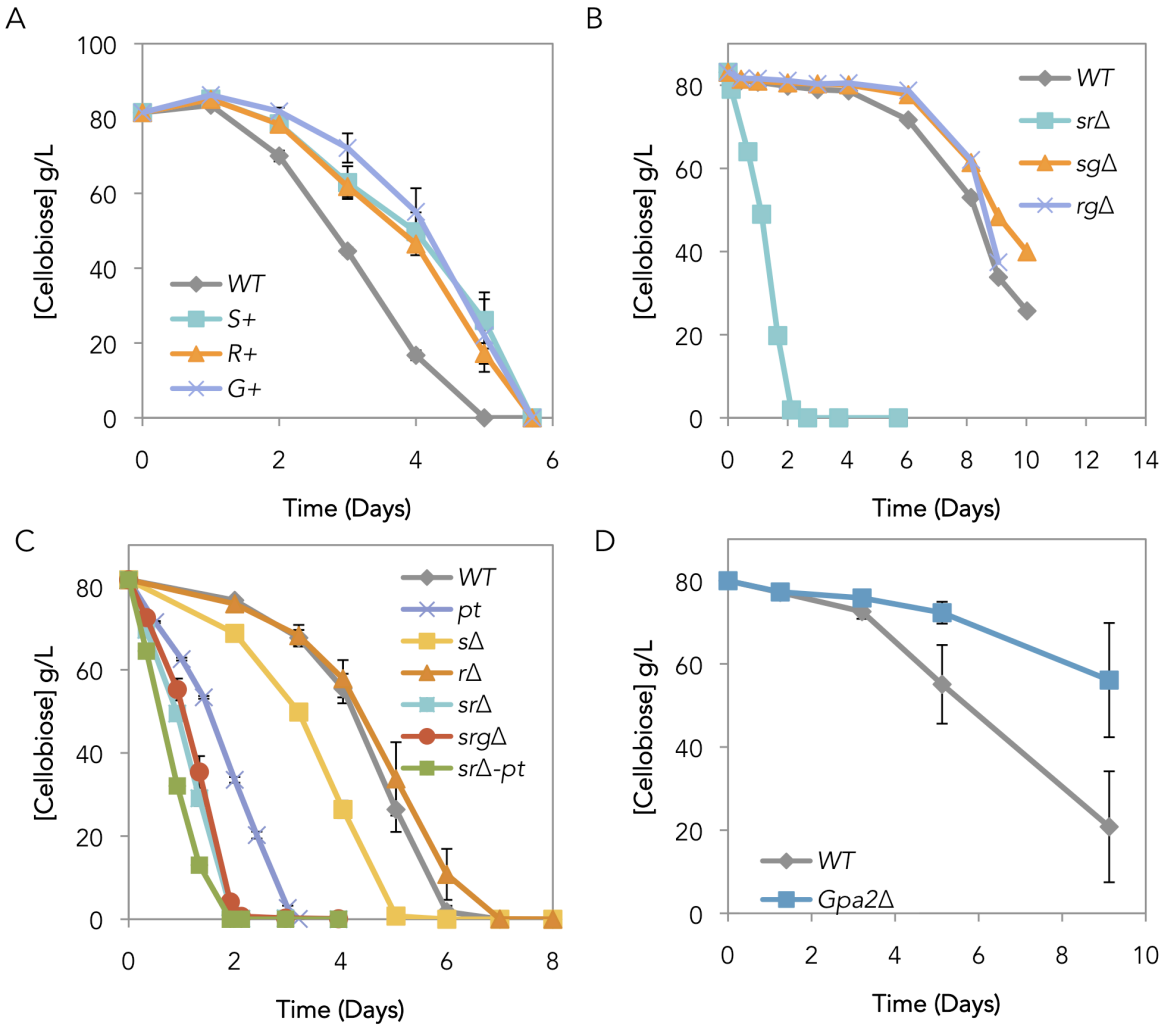

Figure S1. Cellobiose consumption profiles and efficiency of Snf3, Rgt2 and Gpa2 mutants. (A) Cellobiose consumption profiles of strains with consitutively active Snf3 (R229K), Rgt2 (R231K) and Gpa2 (R273A). (B) Cellobiose consumption profiles of *SNF3*, *RGT2*, and *GPA2* double deletion combinations. (C) Cellobiose consumption profiles of *SNF3* and *RGT2* single deletion in comparison to the *srΔ, srgΔ and srΔ-pt* strains. (D) Cellobiose consumption profiles of *GPA2* deletion (*gΔ)* in comparison to the WT strain. In panels A, B, C, and D, the results of 3 biological replicates are shown.

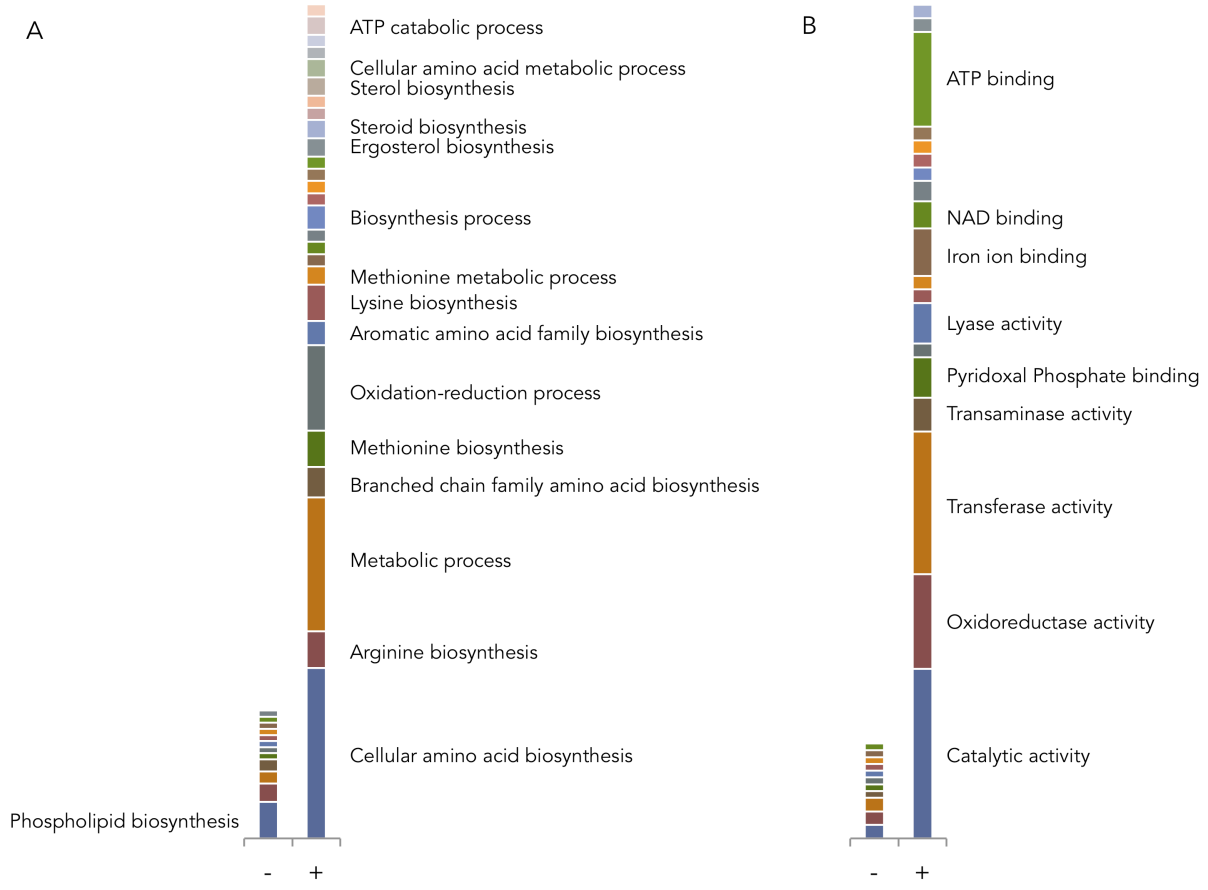

Figure S2. Functional classification of genes uniquely expressed in the *sr*Δ strain. (A) Classification based on GO Biological Processes. (B) Classification based on Molecular Function. The symbol – denotes genes which were uniquely downregulated and + denotes genes which were uniquely upregulated in *sr*Δ. Catagories shown are those with more than two genes detected in the cluster. Dataset 1.6 contains complete classifications of the cluster.

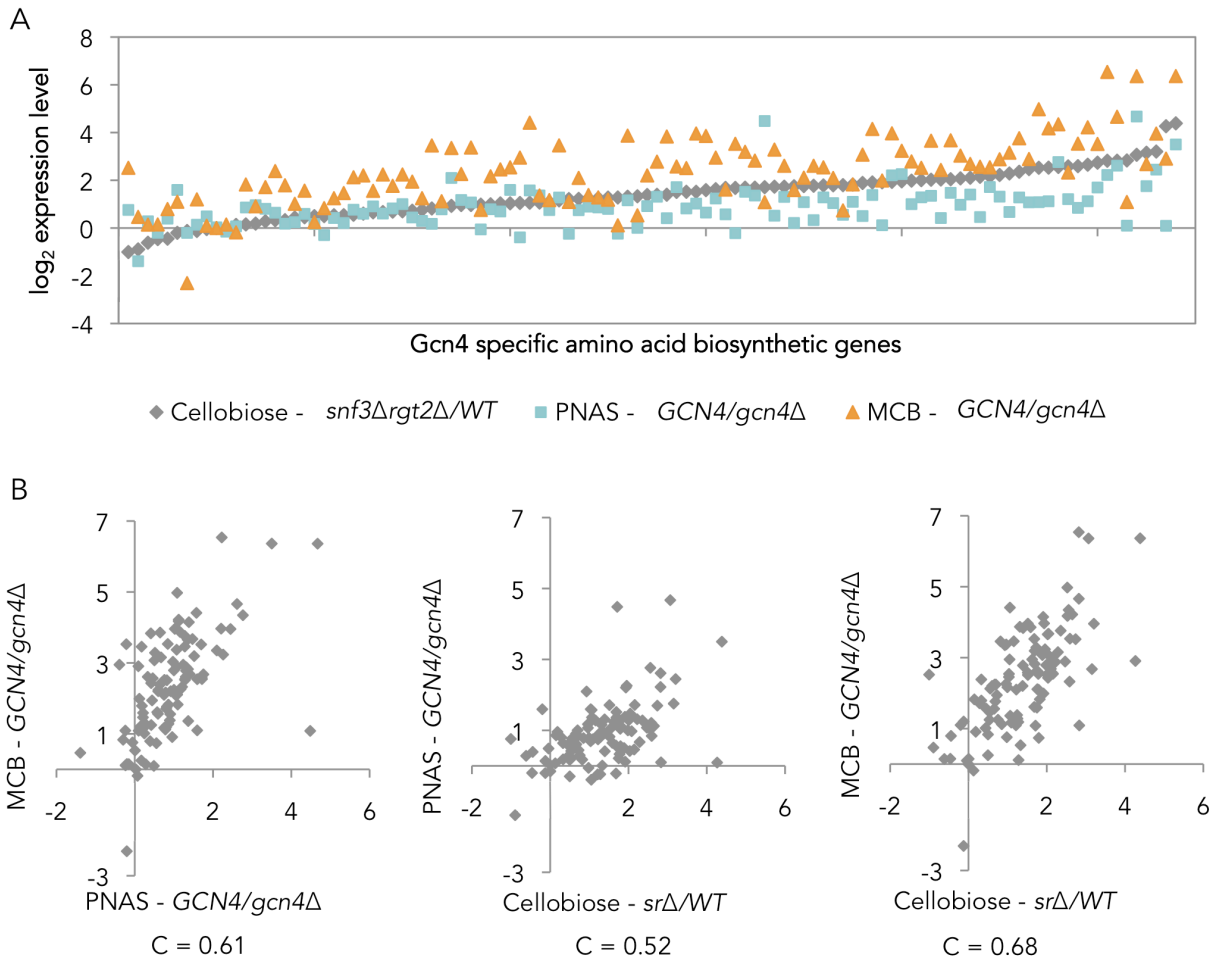

732

733 **Figure S3. Gcn4-specific amino acid biosynthetic gene comparison.** (A) Differential

734 expressional levels of strains from this study (*snf3*Δ*rgt2*Δ/WT) in comparison to

735 *GCN4*/*gcn4*Δ from Moxley *et al.,* 2009 (PNAS) (Moxley *et al*, 2009) and Natarajan *et al.,*

736 2001 (MCB) (Natarajan *et al*, 2001) studies. (B) Pairwise plot of expression levels from

737 three studies and their correlations.

738

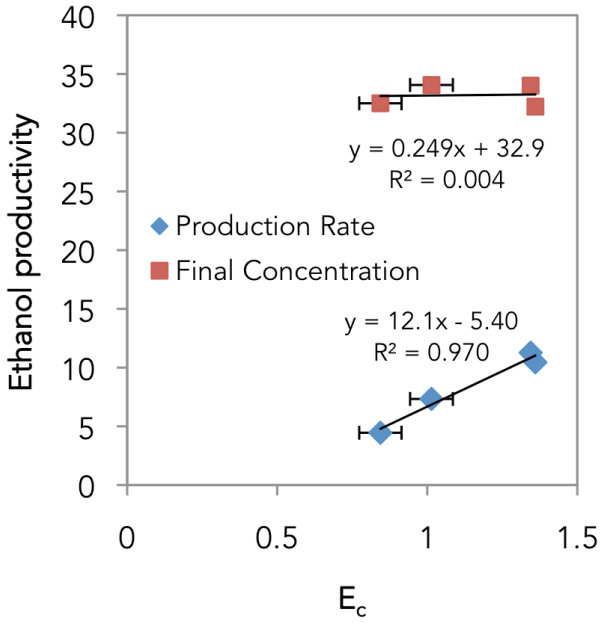

738

739 **Figure S4. Relationship of ethanol productivity parameters and cellobiose**

740 **consumption efficiency (E_c).** Ethanol production rate and the final concentration of

741 ethanol are plotted against E_c.